



## High Voltage Pulse Anodization of a NiTi Shape Memory Alloy

Jin Kawakita,<sup>a,z</sup> Martin Stratmann,<sup>b,\*</sup> and Achim Walter Hassel<sup>b,\*\*</sup>

<sup>a</sup>National Institute for Materials Science, 1-2-1, Sengen, Tsukuba 305-0047, Japan

<sup>b</sup>Max-Planck-Institut für Eisenforschung, D-40237, Düsseldorf, Germany

In an attempt to improve the corrosion resistance of a NiTi shape memory alloy, thick oxide films were fabricated on the surface by an anodic oxidation process. High-voltage square pulse anodization was carried out in various electrolytes over the whole range of pH values from sulfuric acid, acetate buffer, ammonium pentaborate, sodium diphospho heptoxide, sodium aluminate, and potassium hydroxide. Microscopic observation showed that the films are porous or tile structured in nature and the structural analyses by X-ray diffraction and Raman spectroscopy demonstrated their amorphous nature. From the chemical analyses, the oxide films were determined to consist mainly of titanium as the metal component, whereas the nickel content of the oxide films depends on the pH value of the electrolyte as well as the amount of anions incorporated from the electrolyte. The application of an asymmetrical rectangle waveform was effective in increasing the density of the films. An electrochemical technique was used for screening the corrosion resistance of the anodized films and demonstrating the improvement in the resistance against localized corrosion of NiTi.

© 2007 The Electrochemical Society. [DOI: 10.1149/1.2720768] All rights reserved.

Manuscript submitted August 30, 2006; revised manuscript received January 31, 2007. Available electronically April 17, 2007.

Shape memory alloys (SMA) have unique mechanical properties such as pseudo-elasticity or shape memory effect. SMAs are promising materials to develop state-of-the-art devices in the medical or dental field.<sup>1,2</sup> Typical applications are stents for the expansion of coronary arteries or as orthodontic fasteners. Another application is a staple for broken bones which needs to keep its shape during insertion, and then the shape memory effect of the alloys becomes useful for fastening separate bones tightly and to accelerate the healing process. A famous application is the use as a frame for eye-glasses. 50 atom % Ni-50 atom % Ti is suitable because of its transformation around room temperature. However, nickel as a major component is known to cause allergic reactions in the human body of sensitized persons.

NiTi shows a risk of nickel release after implantation.<sup>3,4</sup> Therefore, surface modifications are necessary to hinder dissolution of nickel from NiTi for medical applications, especially in the physiological environment. So far, several kinds of surface treatments have been examined, such as chemical or electrochemical processing,<sup>5,6</sup> heat-treatment, ion implantation, and shot peening.<sup>7-9</sup> An overview of methods useful for the surface treatment of NiTi was recently given in Ref. 10.

A passivation step, e.g., with nitric acid, is often used. When a mechanical load such as bending is applied to a passivated SMA in the human body, the thin and dense passive oxide film cannot follow the strain of the SMA and will therefore be fractured with respect to its brittle nature, conceivably leading to a release of Ni. A porous structure would enable the oxide to adapt to such a strain, to some extent. In addition, thick oxide films may store Ni as re-precipitates within a long percolation path. Therefore, the formation of a thick and porous film of titanium oxide was investigated in this study. Some researchers succeeded in making thick titanium oxide films on pure titanium and titanium alloys by anodizing.<sup>11,12</sup> In this paper, the high-voltage anodization was studied to form a thick and porous oxide film on NiTi. However, a concurrent Ni oxide formation must be expected, as Ni accounts for half the atoms in the alloy and thus oxygen evolution would be a side reaction that results from electronic resistance that is lowered by the Ni in the oxide. Therefore, the effect of the electrolyte composition, supply voltage, time duration, and impressed waveform on the characteristics of oxide was investigated in this paper.

### Experimental

High-voltage anodization was carried out in a two-electrode system. Wires (0.8 mm diam) and disks (10 mm diam) of NiTi (55:45

or 50:50 in atomic ratio) were used as working electrodes. The latter were produced from rods with a diameter of 20 mm which were turned down to 10 mm to ensure probing the homogeneous center composition only. Disks with a diameter of 10 mm were cut from these thinned rods.

The counter electrode was a gold plate with a surface area of 2 cm<sup>2</sup>. Buffer solutions of 0.1 M acetic acid/sodium acetate (pH 4.0) and 0.1 M ammonium pentaborate (pH 8.3) were used at 10°C as electrolytes. In addition, 0.1 M sulfuric acid and alkaline solutions composed of 0.03 M Na<sub>4</sub>P<sub>2</sub>O<sub>7</sub> and 0.0178 M KOH and 0.06 M NaAlO<sub>2</sub> were examined.

In this study, a pulse waveform with a square shape was applied upon anodizing current to suppress oxygen evolution as side reaction on the working electrode during the high-voltage anodization and to form a finely stacked structure of resulting oxides, as it is observed on aluminum after pulse anodization.<sup>13</sup> The ac power source used in this study was a Hewlett Packard 6811A Sourcemeter. The duration of applied current (on-time) and duration of intermission (off-time) in one period were set from 500 μs to 5 ms and 500 μs to 25 ms, respectively. Voltages between 5 and 150 V were applied. The overall anodization time was set between 1 and 55 min.

To characterize the crystallographic properties of the anodized specimens, X-ray diffraction (XRD) and Raman spectroscopic measurements were carried out under grazing incidence (0.5 degree in incident angle) on an X-ray diffractometer (Bruker AXS D8) and a confocal Raman microscope manufactured by Dilor, respectively. Field-emission scanning electron microscopy (FESEM) was carried out with a Leo Gemini apparatus (VP 1550) to visualize the surface structures obtained during anodization of the NiTi. The chemical composition was determined with an energy dispersive X-ray analyzer (EDX) attached to that microscope. For cross-sectional observations, the specimens were embedded into epoxy resin and cross sections were prepared in a metallographic process. X-ray photoelectron spectroscopy (XPS) was carried out to determine the chemical state of the constituent elements of the anodized specimens of NiTi disk with a Physical Electronics Quantum 2000 scanning ESCA microprobe with Al Kα radiation at an acceleration voltage of 25 kV. XPS depth profiles of the specimens were obtained by sputtering the sample with Ar<sup>+</sup> ions.

The electrochemical measurements were carried out with a conventional three-electrode system for investigating the corrosion behavior of the specimens. The test specimens were used as working electrodes. The counter electrode was a gold plate with a surface area of 2 cm<sup>2</sup>. The reference electrode was a commercial Ag/AgCl/3 M KCl type. The electrolyte was a 0.9 wt % NaCl solution at ambient temperature. Dynamic polarization measurements were carried out at a scan rate of 5 mV s<sup>-1</sup> with an electrochemical instrument (VoltaLab Analytical Voltammetry PST050).

\* Electrochemical Society Fellow.

\*\* Electrochemical Society Active Member.

<sup>z</sup> KAWAKITA.Jin@nims.go.jp

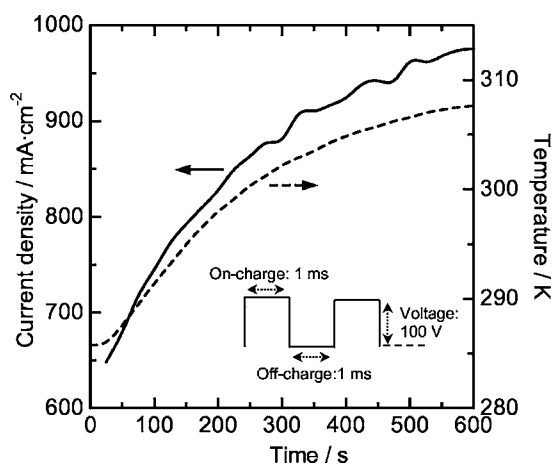
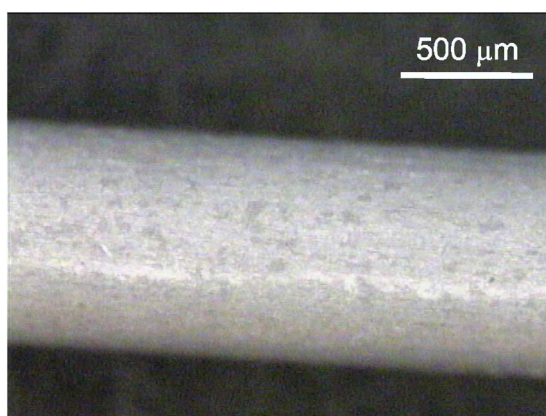


**Figure 1.** Changes in net current and temperature as a function of time during anodization in acetate buffer solution. Inset shows pulse waveform at one period of 1 ms-on and 1 ms-off.

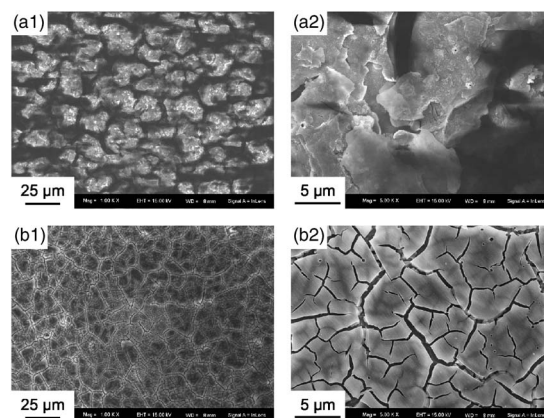
### Results and Discussion

Figure 1 shows typical transients of current and electrolyte temperature during anodization of a NiTi sample for 10 min in an acetate buffer solution. Although similar tendencies of both curves were observed also in a borate buffer solution, the current value was twice as large as and the electrolyte temperature was almost as high as those in the case of the acetate buffer solution. The difference in current between the two solutions was due to the specific resistivity of the solutions (acetate:  $100 \Omega \cdot \text{cm}$ , borate:  $50 \Omega \cdot \text{cm}$  in this study). The increase in temperature is attributed to the Joule heating of the electrolyte resistance. Note that the electrolytic cell was constantly thermostatted and that the increase in temperature occurred even under continuous cooling. It is seen that the current density follows the same trend as the temperature. It is known that the rate of an electrochemical reaction depends on the resistance of the electrolyte<sup>14</sup> and that of the oxide film.<sup>15</sup> The increase in current is therefore attributed to the enhancement of the reaction rate by the increase in electrolyte temperature. The current transient itself does not show that of a typical self-inhibiting process with decaying current. However, a significant contribution must be expected from the reversible charging and discharging of the dielectric film.

Figure 2 shows photographs of the NiTi surface as it appears after anodization. Homogeneous white anodization products were formed on the specimen surface when formed in borate or acetate



**Figure 2.** Appearance of a NiTi surface film formed by anodization at one period of 1 ms on-charge and 1 ms off-charge in acetate buffer solution for 10 min.

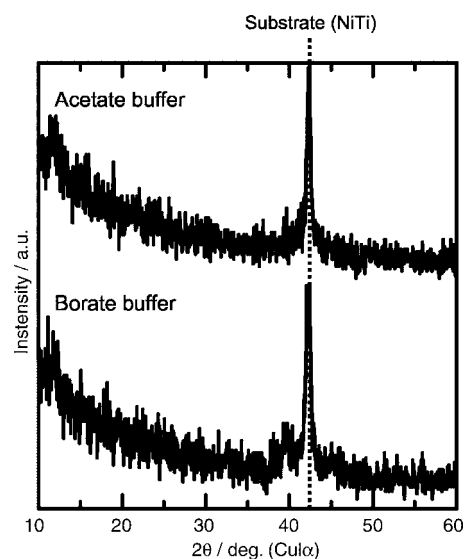


**Figure 3.** Appearance of films on NiTi surface formed by anodization at one period of 1 ms on-charge and 1 ms off-charge in (a) borate and (b) acetate buffer solutions for 10 min.

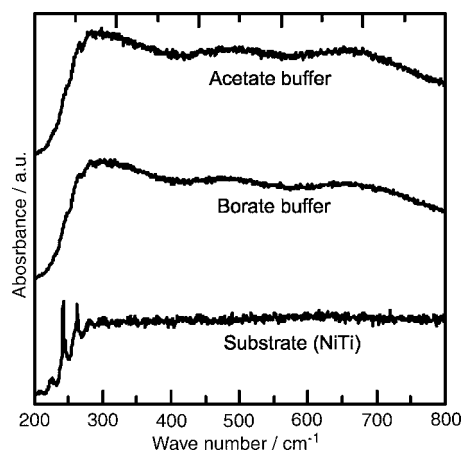
buffer solutions. The lower the applied voltage and the shorter the anodization time, the greater the metallic luster on the anodized specimens. Proper anodizing conditions were determined to be a voltage of 50 V in borate buffer solution and 100 V in acetate buffer for 5 min in one on-charge time period. No thick oxide films could be formed on the NiTi surface in sulfuric acid because of the existence of titanium and nickel as cation in this solution. In an alkaline solution, on the other hand, the formation of a film was not seen to take place because of a continuous exfoliation of the anodization products from the specimen surface.

Figure 3 shows magnified SEM images of the films obtained by anodization of NiTi. Homogeneous cracks are seen in the films formed. This can be attributed to the formation of pathways for oxygen evolution during anodization or a shrinkage of the anodization products during dry-up in air after removal from the electrolyte. The difference in morphology of the anodization products between borate and acetate solutions might be caused by differences in the stability of Ni oxide or hydroxide in these different pH-values.

Figure 4 shows the XRD pattern of the anodization products on NiTi. For angles between  $10^\circ$  and  $60^\circ$ , only one prominent peak is found at an angle of  $42.3^\circ$ . This diffraction line cannot be assigned



**Figure 4.** XRD patterns of films on NiTi surface formed by anodization at one period of 1 ms on-charge and 1 ms off-charge for 10 min in different solutions.



**Figure 5.** Raman spectra of films on NiTi surface formed by anodization at one period of 1 ms on-charge and 1 ms off-charge for 10 min in different solutions.

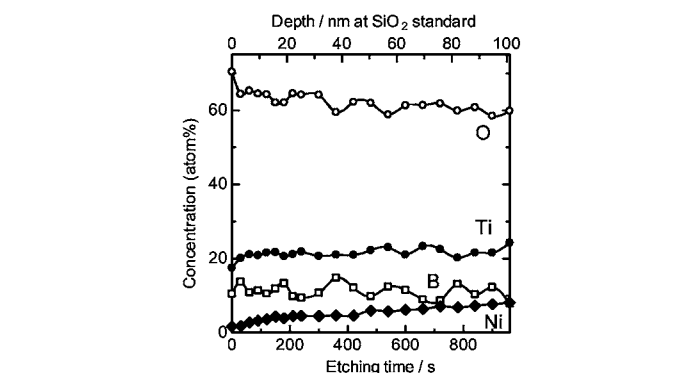
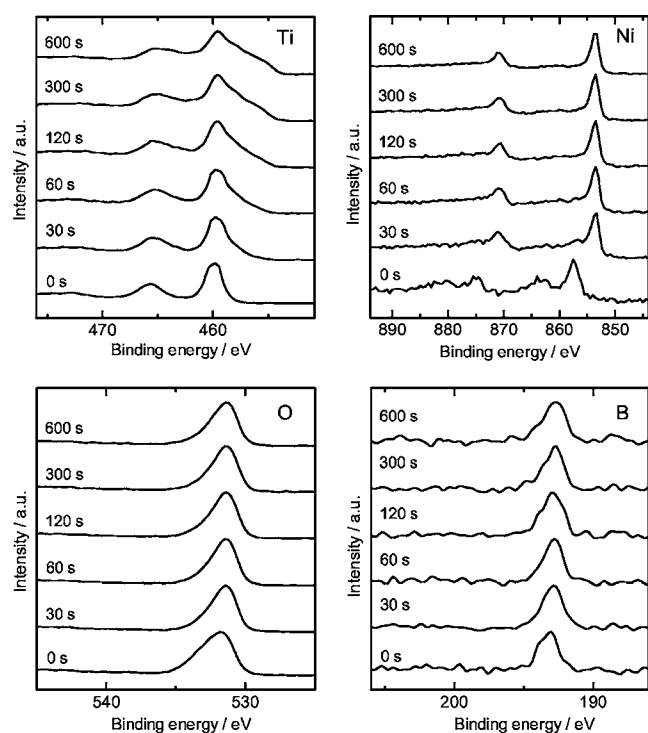


**Figure 6.** XPS spectra and depth profile of a film on NiTi surface formed by anodization at one period of 0.5 ms on-charge and 0.5 ms off-charge in borate buffer solution for 10 min.

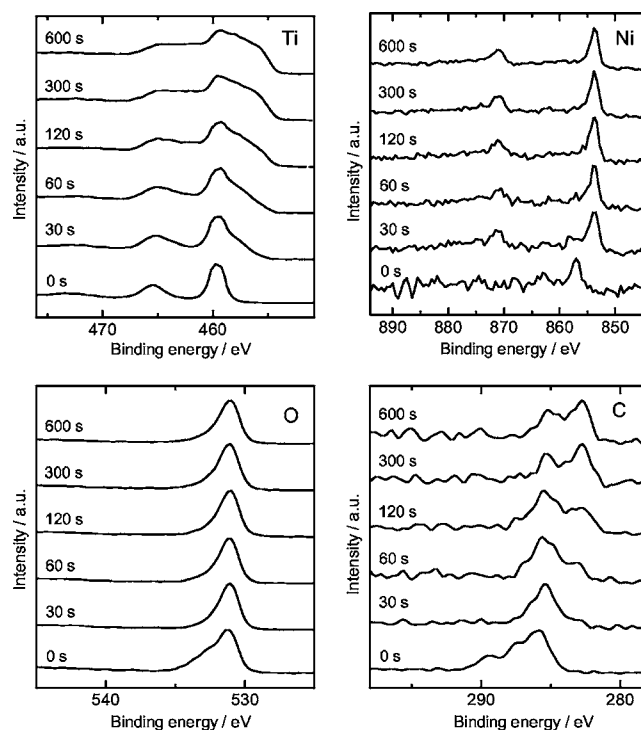


**Figure 7.** XPS spectra and depth profile of a film on NiTi surface formed by anodization at one period of 0.5 ms on-charge and 0.5 ms off-charge in acetate buffer solution for 10 min.

to any oxide but to the NiTi substrate itself. All of the diffraction lines obtained correspond to those of NiTi alloy described in the literature.<sup>16</sup> The peak can be clearly assigned to the prominent 110 peak of the austenite phase. The same pattern was obtained for all specimens prepared under various anodizing conditions. This result indicates that the films are amorphous in structure.

Raman spectra of the anodization products are shown in Fig. 5. No characteristic peaks for either of the three titanium dioxide modifications, rutile, anatase, or brookite, were found. Similar Raman spectra were obtained for all specimens prepared under various conditions. These two results regarding the crystallography of the anodization products prepared on NiTi demonstrate that the oxide formed by anodization is amorphous regardless of the type of electrolyte used.

Figures 6 and 7 compare the typical XPS spectra of the films obtained by anodizing. The shape of all peaks remained almost similar during Ar<sup>+</sup> sputtering for more than 600 s, indicating the homogeneous composition. In addition, anions such as CH<sub>3</sub>COO<sup>-</sup> or B<sub>5</sub>O<sub>8</sub><sup>-</sup> could be incorporated into the oxide from the electrolyte. From the analysis of the XPS depth profiles for sputter times between 600 and 960 s, the average chemical composition of the films were determined, as listed in Table I. Under both anodizing condi-

**Table I. Chemical composition (atom %) of anodization products on NiTi obtained by anodization determined by XPS.**

Electrolyte	Ti	Ni	O	B	C
Borate	21.58	7.07	60.03	11.32	—
Acetate	27.00	2.12	64.48	—	6.40

tions, titanium is the main metal component in the oxide film and the content of Ni is suppressed to 2.12% in the acetate buffer, i.e., decreasing the pH value. The upper limit for the content of electrolyte species was approximately 10%, assuming that the electrolyte species ( $B_5O_8^-$  and  $CH_3COO^-$ ) kept the chemical formula in the films.

Cross sections were prepared from these anodized NiTi specimens. The porous nature of the formed oxide is shown in Fig. 8. The film had grown to a thickness of 5  $\mu\text{m}$  after 10 min of anodization with a symmetric duty cycle of 1 ms. The film thickness depended on the total on-charge time. This corresponds to a growth rate of about 8  $\text{nm s}^{-1}$ , under a simplifying assumption of constant growth rate. The porous structure is most likely a result of the strong oxygen evolution during high-voltage anodization of the film. Cracks were observed in the films, implying the presence of stress from the heavy oxygen gas evolution. The chemical composition of these specimens as determined by EDX is compared in Table II. Similar to the result of XPS, a dependence of the chemical composition of the oxide on the electrolyte used was found. Moreover, it was found that the composition of the oxide films over their thickness is quite homogeneous. Figures 9 and 10 show cross-sectional views of the oxide films fabricated in the same electrolyte but under variation of the anodizing conditions. Figure 9 indicates the effect of the on-charge time on the formation of the oxide films. When the on-charge time during anodization was short, the particles of the oxide film had a less-cracked structure. This is attributed to the difference in stress in the oxide particles during anodization. For a short on-charge time, a

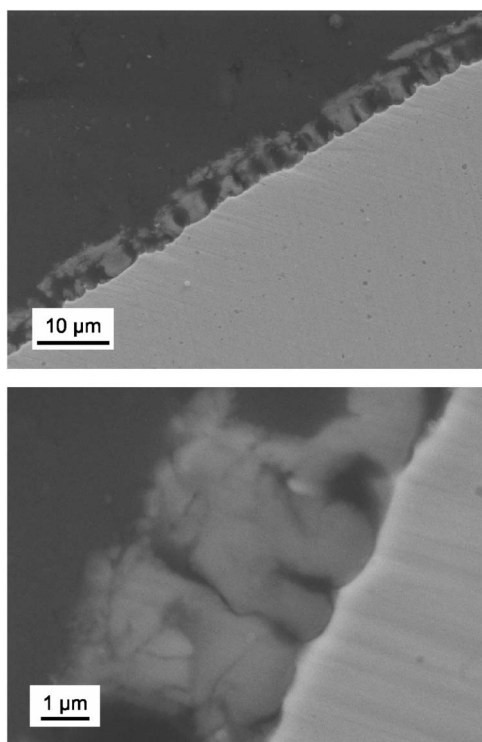


**Figure 8.** Cross-sectional views of NiTi specimen formed by anodization at one period of 1 ms on-charge and 1 ms off-charge in acetate buffer solutions for 10 min.

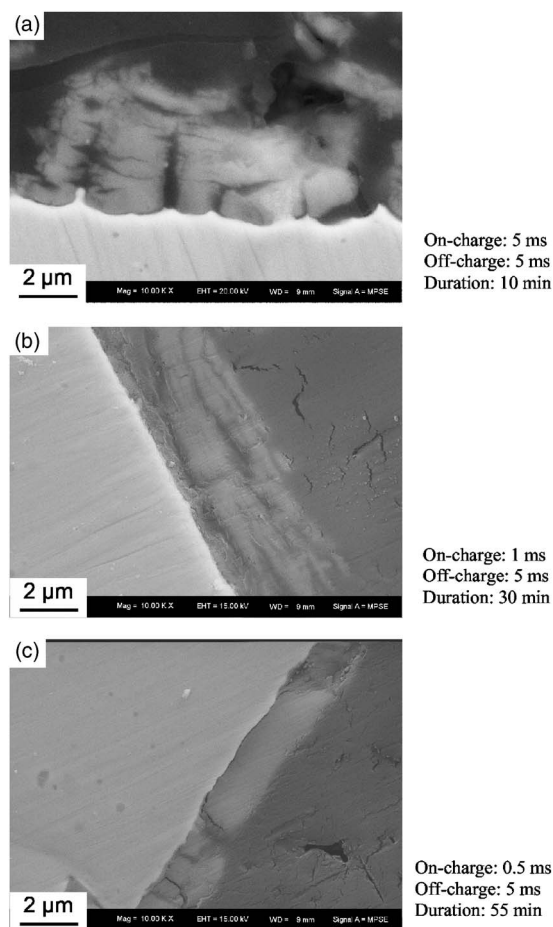


**Figure 9.** Cross-sectional views of NiTi specimen formed by anodization at one period of on-charge for (a) 5, (b) 1, and (c) 0.5 ms and off-charge for 5 ms in acetate buffer solution in total on-charge time of 5 min.

discontinuous growth of the oxide and thus a lower volume of oxygen bubbles could relax the stress applied to the oxide particles. When the on-time during anodization was short, the particles composed of the oxide film had a less-cracked structure. Figure 10 indicates the effect of the off-charge time on the formation of oxide films for a fixed on-charge time. When the off-charge time during anodization was longer, the film structure became denser, especially near the interface. This is again attributed to the effect of oxygen bubbles during formation of the oxide film. An extended off-charge time allows the bubbles to detach from the NiTi substrate or to dissolve in the solution.

To get a first idea of the degree of corrosion protection improvement polarization curves were recorded on differently prepared NiTi samples. Figure 11 compares the polarization curves of NiTi specimens in 0.9% NaCl aqueous solution at a scan rate of 5  $\text{mV s}^{-1}$ . Regarding the potential where the anodic current rapidly increased in the polarization curve, the high voltage anodized NiTi was shifted significantly to more noble values as compared to the abraded specimen or a specimen with passivation at low voltage. During this polarization tests, the nontreated and the passivated NiTi specimens

**Table II. Chemical composition (atom %) of anodization products on NiTi obtained by anodization determined by EDAX.**

Electrolyte	Ti	Ni	O
Borate	26.38	8.12	65.51
Acetate	29.24	3.84	66.92

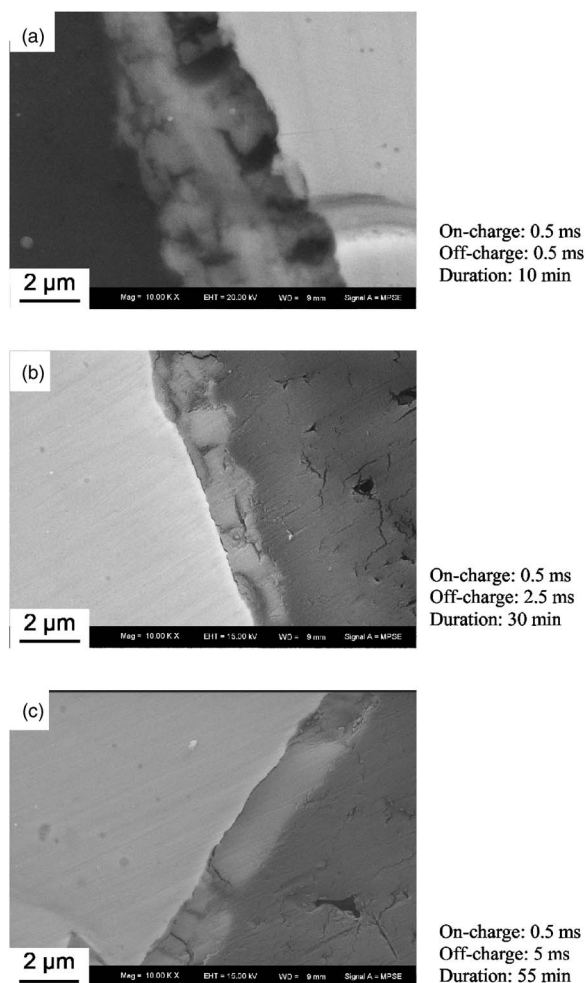


**Figure 10.** Cross-sectional views of NiTi specimen formed by anodization at one period of on-charge for 0.5 ms and off-charge for (a) 0.5, (b) 2.5, and (c) 5 ms in acetate buffer solution in total on-charge time of 5 min.

were heavily attacked by pitting corrosion. The high-voltage-anodized NiTi showed only oxygen evolution. The noble shift of the potential at which the current increases steeply, for the pulse anodized specimens was mainly because of a kind of barrier behavior of thick oxide films formed on the NiTi surface. Fluctuations of the current, however, were observed for the anodized specimens in the potential region less noble than the electrode potential at which the current increased rapidly. This may be caused by a localized corrosion at the interface between the oxide film and the substrate, as the porous oxide film can be easily penetrated by the solution. As mentioned above, however, the denser oxide film was formed under the longer off-time condition (see Fig. 10). The denser oxide film has lower current peaks than the porous one in the potential range with the current fluctuation, as clearly seen in the inset of Fig. 11. The increase in density of the oxide film by a proper adjustment of the anodizing parameters could suppress such a phenomenon of localized corrosion.

### Conclusions

Thick oxide films  $\sim 5 \mu\text{m}$  thick were formed on NiTi shape memory alloys by high voltage anodization with voltages between 5 and 150 V using a pulse waveform. The duration of the applied current (on-time) and duration of intermission (off-time) in one period were varied from 500  $\mu\text{s}$  to 5 ms and 500  $\mu\text{s}$  to 25 ms, respectively, and the overall anodization time was set to between 1 and 55 min.

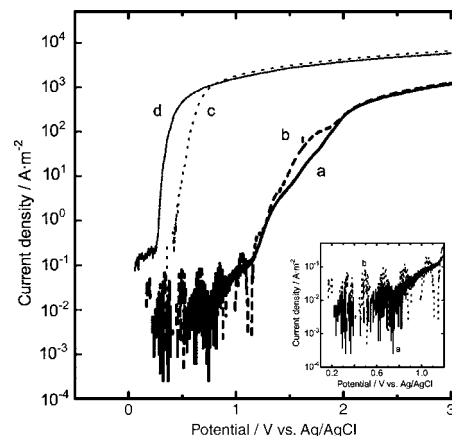


**Figure 11.** Polarization curves of NiTi specimens in 0.9% NaCl aqueous solution at 5 mV/s, (a) —: anodized at 0.5 ms (ON) and 5 ms (OFF) for 10 min in acetate buffer, (b) ---: anodized at 0.5 ms (ON) and 0.5 ms (OFF) for 10 min in acetate buffer, (c) ····: passivated at 3 V for 10 min in acetate buffer, and (d) -·-·: abraded.

The amorphous structure of the oxides formed was confirmed by both XRD and Raman spectroscopy. Investigations into the porous structure were performed by cross-sectioning. The porous structure could be varied by controlling the anodizing conditions such as the pulse waveform and duty cycle. The anodizing procedure described here is a promising route for the formation of strain tolerant surface oxides as they are required by a metallic substrate such as NiTi.

The oxides were mainly composed of titanium oxide. The nickel content could be suppressed to about 2% in the oxide. As for low voltage anodization, some amount of the electrolyte anions were incorporated in the oxide.

The corrosion resistance of NiTi in chloride solution was improved by the anodizing treatment introduced in this study. This is a promising result in terms of implant application of NiTi.

### Acknowledgments

The financial assistance through a fellowship of the Ministry of Education, Culture, Sports, Science and Technology of Japan for J.K. is gratefully acknowledged.

*Max-Planck-Institut für Eisenforschung assisted in meeting the publication costs of this article.*

### References

1. P. Filip, J. Lausmaa, J. Musialek, and K. Mazanec, *Biomaterials*, **22**, 2131 (2001).
2. L. G. Machado and M. A. Savi, *Braz. J. Med. Biol. Res.*, **36**, 682 (2003).
3. R. Venugopalan and C. Trépanier, *Minimally Invasive Ther. Allied Technol.*, **9**, 67 (2000).
4. M. Es-Souni, M. Es-Souni, and H. Fisher-Brandies, *Anal. Bioanal. Chem.*, **381**, 557 (2005).
5. S. Barison, S. Cattarin, S. Daolio, M. Musiani, and A. Tuissi, *Electrochim. Acta*, **50**, 11 (2004).
6. K. Fushimi, M. Stratmann, and A. W. Hassel, *Electrochim. Acta*, **5**, 1290 (2006).
7. S. M. Green, D. M. Grant, and J. V. Wood, *Mater. Sci. Eng., A*, **224**, 21 (1997).
8. S. A. Shabalovskaya, *Biomed. Mater. Eng.*, **12**, 69 (2002).
9. G. S. Firstov, R. G. Vitchev, H. Kumar, B. Blanpain, and J. V. Humbeeck, *Biomaterials*, **23**, 4863 (2002).
10. A. W. Hassel, *Minimally Invasive Ther. Allied Technol.*, **13**, 240 (2004).
11. H. Habazaki, M. Uozumi, H. Konno, K. Shimizu, P. Skeldon, and G. E. Thompson, *Corros. Sci.*, **45**, 2063 (2003).
12. T. H. The, A. Berkani, S. Mato, P. Skeldon, G. E. Thompson, H. Habazaki, and K. Shimizu, *Corros. Sci.*, **45**, 2757 (2003).
13. V. Raj, M. R. Rajaram, G. Balasubramanian, S. Vincent, and D. Kanagaraj, *Trans. Inst. Met. Finish.*, **81**, 114 (2003).
14. K. I. Popov, S. S. Djokić, and B. N. Grgur, *Fundamental Aspects of Electrometallurgy*, p. 10, Kluwer Academic/Plenum Publishers, New York (2002).
15. S. Rüße, M. M. Lohrengel, and J. W. Schultze, *Solid State Ionics*, **72**, 29 (1994).
16. R. Schmidt, M. Schlereth, H. Wipf, W. Assmus, and M. Müller, *J. Phys.: Condens. Matter*, **1**, 2473 (1989).